Magnetotransport studies of the single and bilayer two dimensional electron gas in the quantum Hall regime

Galistu, G.M.

Publication date
2010

4. Critical behavior

4.1 Introduction

During the last two decades, following the discovery of the quantum Hall effect by von Klitzing *et al.* [1] and the pioneering work on quantum criticality of the PP-transitions by Wei *et al*. [2a-3], a host of experimental work has been done in order to shed light on the exact nature of scaling in the quantum Hall regime at low temperatures. The principal objective is to establish the following scaling laws for the experimentally observed Hall resistance R_{H} and the longitudinal resistance R_0 with varying magnetic field B and temperature T [2b]

$$R_{H,0} = F_{H,0}(\Delta B, T^{-\kappa}) \tag{4.1}$$

Here, $\Delta B = B - B^*$ is the magnetic field relative to the critical value B^* which corresponds to the center of a Landau band. The critical exponent κ equals the ratio

$$\kappa = p / 2\nu_0 \tag{4.2}$$

with ν_0 denoting the localization length exponent of the 2DEG and p is a finite temperature exponent determined by inelastic scattering. *Eq*. (4.3) determines the maximum slope of the Hall resistance R_{H} with varying B to diverge algebraically as T goes to zero according to

$$\left(\frac{\partial R_H}{\partial B}\right)_{\max} \propto T^{-\kappa}. \tag{4.3}$$

Wei *et al.* originally extracted the numerical value $\kappa = 0.42$ from the transport data taken from a low mobility *InP-InGaAs* heterostructure which is independent of the index of the PP transition [2a-3]. Following the renormalization theory of the quantum Hall effect developed by Pruisken [2b] this experimental value was subsequently regarded to be universal.

These remarkable advances have led several groups around the world to investigate the power law of *Eq*. (4.3) for a variety of different but otherwise arbitrarily chosen laboratory samples [4-7]. A range of different values for κ were measured, however, varying from 0.3 to 0.9. The difficulty in experimentally establishing universality of the PP transition has

caused the quantum Hall community to split up into two different groups with entirely different physical objectives each.

4.1.1 The 'H.P. Wei' school of thought

The first group, briefly termed the 'H.P. Wei group', held on to the general belief that the critical exponent κ is universal. Motivated by the theoretical foundations of scaling established by Pruisken, this group experimentally pursued the universality of not only κ but also the complete scaling functions $F_{\mathrm{H},\,0}$ with varying T and B. It was well understood, however, that universality strictly holds in the limit where T goes to absolute zero. In practice this means that the transport measurements at finite T should be conducted on sufficiently homogeneous samples with potential fluctuations that are short-ranged relative to the magnetic length.

4.1.2 The 'phenomenological' school of thought

Quite unlike the experimental objectives of the H.P. Wei group, the second school of thought, briefly termed the 'phenomenological group', went on in different directions altogether. For example, to explain the differences in the experimental κ; finite size scaling experiments have been conducted that were aimed at disentangling the individual exponents values of p and ν_0. These investigations led to the idea that the exponent p, unlike the localization length exponent ν_0, is a material dependent parameter that varies not only from sample to sample but also from Landau level to Landau level.

At a much later stage, experiments conducted on a new class of high quality samples indicated yet a very different behavior. Rather than a *power law* in T, the transport data were now fitted to a semi classical '*linear law.'* (Shahar *et al*. [8]) This kind of data fitting clearly does not teach us anything about the phenomenon of Anderson localization and fundamentally upsets the entire idea of quantum criticality in the quantum Hall regime.

At the time of this writing, the various conflicting results and ideas advocated by the 'phenomenological school of thought' seem to have lost most of its support in the literature. What has in general been overlooked by this group is that the transport data taken from arbitrary samples at finite T do not necessarily reveal the true (scaling) behavior of the

2DEG in the limit $T = 0$. It may therefore not be a complete surprise to know that the most important advances in the field have emerged from entirely different sources.

4.1.3 The PI transition

First, there is the longstanding experimental problem of how to disentangle the effects of macroscopic sample inhomogeneity from the intrinsic transport properties of the 2DEG. In brief, it has turned out that defects such as small gradients in the electron density can cause major aberrations in the extraction of κ from the PP transitions [11-14]. These as well as other kinds of defects such as contact misalignment have a much less dramatic impact when the measurements are conducted on the PI transition. Subsequently, the PI transition became the primary focus of experimental interest.

The most important conclusions drawn from the experiments on the PI transition can be found in *Refs* [15,16]. Unlike the 'generally accepted' exponent value $\kappa = 0.42$ previously obtained from three different PP transitions of an *InP-InGaAs* heterostructure, the *correct* experimental value extracted from the PI transition of the same sample turns out to be $\kappa = 0.57$. The difference between these two experimental estimates can be explained based on density gradients that dramatically complicate the experiment on the PP transition but do not affect the κ taken from the PI transition.

The detailed studies on the PI transition furthermore revealed universal scaling functions for the longitudinal conductance σ_0 and the Hall conductance σ_H. These scaling functions, when plotted as T-driven flow lines in the σ_0-σ_H conductance plane, display all the fundamental features of scaling that previously could not be observed from the data taken from the PP transitions. As pointed out in the original papers, these findings provide important information on the unification of the fractional quantum Hall effects based on composite fermion theory, in particular, the cross-over between the half-integral Fermi-liquid state and the quantum critical state.

Even though the advances made on the PI transition have resolved many longstanding controversies in the field, several major experimental difficulties have nevertheless remained. For example, since not much is known about the microscopic details of the low mobility *InP-InGaAs* heterostructure it is unclear whether the criteria for a homogeneous, short ranged random potential are being satisfied. The random alloy scattering in these

samples may, in fact, exhibit long-ranged components relative to the magnetic length. This would mean that the newly extracted value of $\kappa = 0.57$ is, in fact, an effective exponent and even lower temperatures are needed in order to be able to extract the much sought-after critical value.

4.1.4 Numerical value of κ

This takes us to the second important advance more recently made by the Princeton group of D.C. Tsui who investigated the PP transitions taken from a set of specially grown state-of-the-art $Al_xGaAs/Al_{0.33}Ga_{0.67}As$ heterostructures with different *Al* concentration *x* [17,18]. By varying *x* one effectively varies the range of the potential fluctuations in these otherwise extremely homogeneous samples. For example, for small values of *x* the *Al* atoms are all distant apart from each other and the disorder potential is predominantly *long- ranged*. On the other hand, by increasing the concentration *x* the *Al* atoms come closer together and the random potential fluctuations become predominantly *short-ranged*. Upon further increasing the concentration *x* the *Al* atoms are believed to form clusters. This clustering takes place over distances which are large relative to the magnetic length and, hence, the randomness becomes *long-ranged* again.

The experimental values for κ extracted for different values of *x* generally exceed the value 0.42. However, when the criteria for *short range* potential fluctuations were met D.C. Tsui *et al.* measured a value of $\kappa = 0.42$ in the temperature range from10 to 1000 mK. This experimental value - which surprisingly coincides with the original but incorrect result of H.P. Wei *et al*. - is now believed to be the correct universal value of κ. These impressive findings by the Princeton group unequivocally demonstrate the existence of quantum criticality in the quantum Hall regime and, hence, the correctness of the `H.P. Wei' school of thought.

4.1.5 Confronting controversies

The advances made on both the PI transition and the critical exponent κ are an important step toward establishing a unified renormalization theory of the quantum Hall effects. At the same time, these advances are a landmark in the theory of Anderson localization and interaction effects. However, the subject matter is still at its infancy and certainly not free of controversies. First of all, it is important to emphasize that the newly established value

of $\kappa = 0.42$ has absolutely nothing to do with the original findings of H.P. Wei *et al.* Unlike the claims made by D.C. Tsui *et al.*, the coincidence is purely accidental thus creating a lot of confusion. The only way to understand the original H.P. Wei result of $\kappa = 0.42$ is by considering the combined effects of both *long ranged* potential fluctuations and macroscopic sample *inhomogeneity*. Whereas the former causes the experimental κ to *increase* from the universal value 0.42 up to the aforementioned value of 0.57, the latter causes κ to *decrease* from 0.57 back to the numerical value 0.42. Notice that this combination of experimental defects typically explains the different values of κ in the range 0.3 – 0.9 previously extracted from arbitrarily chosen samples at finite temperatures.

Secondly, there are the more recent attempts by the Princeton group to disentwine the critical exponents p and ν from the definition of κ in *Eq*. (4.0) [19]. In particular, by studying the scaling of the PP transition with varying sample size L rather than T, the individual exponent values have been extracted and the result is $p = 2$ and $\nu = 2.4$ respectively. Since the localization length exponent ν is numerically the same as the free electron result known from computer simulations, D.C. Tsui *et al.* conclude that the critical behavior of the interacting electron gas and the disordered free electron gas are in the same universality class. According to Pruisken this conclusion is incorrect. In particular, the advances made in the theory of localization and interaction effects have clearly shown that the infinitely ranged Coulomb interaction present in the laboratory sample renders the transport of the 2DEG entirely non-Fermi liquid-like. This transport behavior is characterized by previously unrecognized interaction symmetries (termed F-invariance) as well as distinctly different non-Fermi liquid critical exponent values.

The experimental problem that was discarded by D.C. Tsui *et al.* is that finite size scaling can only be studied if it compares the data taken from *different* samples. However, along with different values of L one also finds that the characteristic length scale L_s and temperature scale T_s for scaling varies from sample to sample in an uncontrolled manner. Unlike κ which is measured on a single sample, there is as of yet no experimental design that warrants an unambiguous measurement of the individual exponent values of p and ν.

Last but not least, the samples used by D.C. Tsui *et al.* do not permit an investigation of the PI transition since that lowest Landau level displays the fractional quantum Hall effect. This most likely complicates the study of macroscopic inhomogeneity effects and, along with that, the subtleties of a unified scaling diagram that incorporates both the integral and

fractional quantum Hall effects. In any case, D.C. Tsui *et al.* do not investigate the universal scaling functions for σ_0 and σ_H and it remains unclear whether the PP transitions of their samples provide access to the *irrelevant* exponents describing the corrections to scaling. Future work probably will tell.

4.1.6 Outline of this Chapter

In this chapter we will present the results of magnetotransport measurements conducted on an InGaAs/GaAs quantum well with a geometrical factor of 1.5 (see *Fig*. 3.11) using four different electron densities (n_e = 1.0, 1.3, 1.8 and 2.0 × 10^{15} m^{-2}). We will consider both the PP and PI transition. Whereas the PP transitions give us the necessary information about the quality of the Hall bar in terms of density gradients, only the PI transition will be used to study quantum criticality.

The analysis of the data is done in much the same way as was done previously in *Refs* [11-14]. The results will be compared with those obtained from a similar quantum well with a geometrical factor of 5.2 in *Ref* [11]. We will discuss the results of numerical simulations and see to what extent the relatively large gradients in the electron density of the 2DEG can explain the deviations found in the curves displaying critical behavior.

Using our experimental results discussed in this Chapter as well as *Chap*. 5 we will construct a *T*-driven flow diagram that displays both relevant and irrelevant critical behavior. We then compare the results with the theoretical predictions on scaling similarly to what was previously done in *Ref.* [15].

4.2 InGaAs/GaAs quantum well with tunable carrier density: PP transition

The InGaAs/GaAs 2DEG used for our magnetotransport measurements has a tunable carrier density. Being insulating in the dark, the electron density in the quantum well can be increased by illuminating the 2DEG with an infrared LED at low temperatures.

The carrier density is an important parameter of the 2DEG since it determines at which values of the magnetic field the quantum Hall transitions occur. By changing the carrier density in the range in which the field-value at which the PI transition occurs is still achievable with our magnet, we can create different sample conditions. This allows us to

check for the universality of the critical exponents. The wafer out of which the Hall bar was prepared has been grown by molecular beam epitaxy (MBE) at the Moscow state university. The 2DEG is located in a 12 nm thick $In_{0.2}Ga_{0.8}As$ layer, separated from the doping layer by a 20 nm thick spacer. Etching of the Hall bar was done using photolithography. The carrier concentration in the sample can be varied smoothly between zero (insulating sample) and $n_e = 4 \times 10^{15}$ m^{-2} with an accuracy better than 1 % [11]. To illuminate the 2DEG we send a current through the LED using a Keithley 2400 current source. The illumination was done stepwise by controlling the pulse duration and slowly increasing the current through the LED. An image of the Hall bar is shown in *Fig*. 3.11 of the previous chapter. The Hall bar has 6 potential and 2 current contacts. Unfortunately one current contact and two potential contacts turned out to be high-Ohmic which reduced the possibility of directly probing the inhomogeneities in the carrier density of the Hall bar. Still there are other methods available to estimate the inhomogeneous nature of the carrier density. These methods have been applied and will be discussed in this chapter. In the following *Figs*. 4.1 a) - d) we will show the resistance- and Hall curves measured DC for the four densities attained after longer and longer illumination. All curves where measured using the DC method described in *Chap* 3.

Figs. 4.1 a) – d) show the expected improvement of the quality of the data with increasing density. For the highest two densities (*Figs*. 4.1 c, d) the small overshoot of the resistivity (ρ_{xy}), at the beginning of the plateaus, still visible in the lowest two densities (*Figs*. 4.1 a, b), disappears. The plateaus become quantized within 0.05 % of the expected values and ρ_{xx} becomes zero between the transitions.

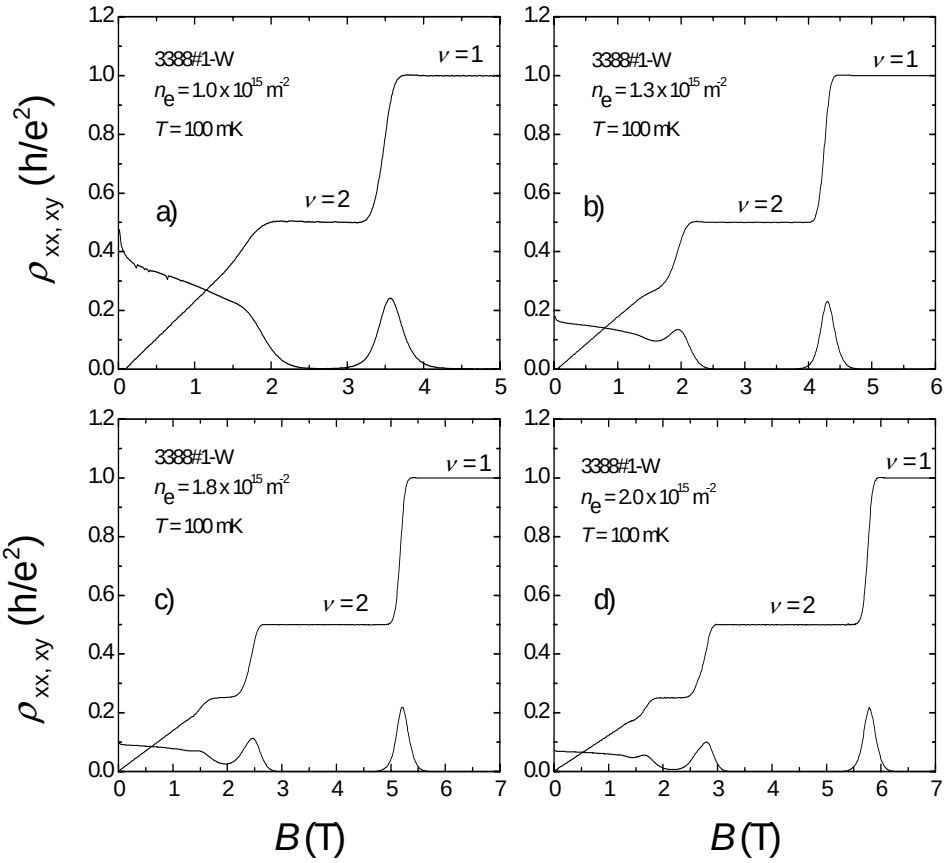

Figure 4.1 Resistance and Hall-curve for a) $n_e = 1.0 \times 10^{15}$ m^{-2}, b) $n_e = 1.3 \times 10^{15}$ m^{-2}, c) $n_e = 1.8 \times 10^{15}$ m^{-2} and d) $n_e = 2.0 \times 10^{15}$ m^{-2}. The measurement current is 10 nA. T = 100 mK.

4.2.1 Determining inhomogeneities

A great obstacle in probing the quantum critical behavior is the inhomogeneous nature of the Hall bar. Inhomogeneities in the electron density of the 2DEG are mainly a result of the growth process of the wafer. The simplest approach to the inhomogeneity problem is a gradient in the electron density throughout the Hall bar. The most harmful consequence of inhomogeneities is that transitions take place at different values of the magnetic field

throughout the 2DEG and make an accurate determination of the scaling behavior impossible. This is especially true for the PP transitions [11]. It is important therefore to be able to make an estimate of the magnitude of this gradient in the electron density. The common way of doing this is to measure the Hall resistance at two places of the Hall-bar. The shift in curves then tells us how large this gradient is. Unfortunately only one pair of Hall contacts and one pair of resistance contacts were present on the Hall-bar. Another way of estimating the magnitude of the gradient is making use of reflection symmetry [11,13]. Reflection symmetry states that the longitudinal resistances measured at both sides of the Hall bar interchange by reversing the polarity of the magnetic field.

$$R^{t}_{xx}(B) = R^{b}_{xx}(-B) \tag{4.4}$$

where *t* and *b* stand for top and bottom respectively. So having only one pair of resistance contacts but measuring for reversed field also, gives us the data for the opposite pair of resistance contacts. It is shown that the longitudinal resistances at the top and bottom of the Hall bar are given by [13]

$$R^{t}_{xx} = \frac{V^{t}_{xx}}{I_x} = \frac{L}{W}(\rho_0 + \alpha\frac{W}{2}) \tag{4.5}$$

and

$$R^{b}_{xx} = \frac{V^{b}_{xx}}{I_x} = \frac{L}{W}(\rho_0 - \alpha\frac{W}{2}) \tag{4.6}$$

where

$$\alpha = \frac{\partial\rho_H}{\partial\nu}\frac{\partial\nu}{\partial x} \tag{4.7}$$

From Eq. (4.2) and (4.3) it follows that

$$R^{t}{}_{xx}(B) - R^{t}{}_{xx}(-B) = \alpha L \tag{4.8}$$

Combining Eq. (4.4) and (4.5) gives

$$R^{t}{}_{xx}(B) - R^{t}{}_{xx}(-B) = \frac{\delta\rho_H}{\delta\nu}\frac{\partial\nu}{\partial x}L \tag{4.9}$$

Zero coordinates (*x, y*) are taken at the center of the Hall bar. *Eq*. (4.9) tells us that the difference of R_{xx} for both field polarities is equal to the slope of the Hall resistivity times the gradient along the total length *L* of the Hall bar. ρ_H is the Hall resistivity for the ideal case without gradient. Since we do not know this value, we approximate it by

$$\rho_H = \frac{R_{xy}(B) + R_{xy}(-B)}{2} \tag{4.10}$$

Plotting our data versus the filling factor ν for the PP-transition $2 \longrightarrow 1$ and applying *Eqs*. (4.9) and (4.10) gives us the ΔR_{xx} and $\delta\rho_H/\delta\nu$ curves for $n_e = 1.0$ and 1.3×10^{15} m^{-2} (*Fig*. 4.2) and $n_e = 1.8$ and 2.0×10^{15} m^{-2} (*Fig*. 4.3).

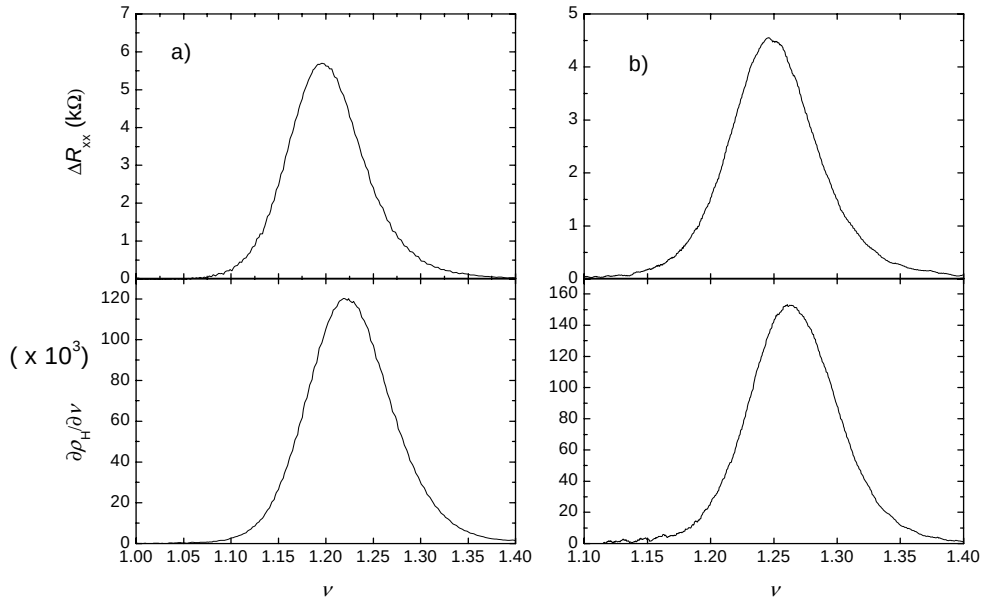

Figure 4.2 ΔR_{xx} for both field polarities (top) and slope of ρ_H versus filling factor (bottom) at $T = 100$ mK for a) $n_e = 1 \times 10^{15}$ m^{-2} and b) $n_e = 1.3 \times 10^{15}$ m^{-2}.

Using *Eq*. 4.9 the ratio of peak values (top/bottom) gives us approximately a gradient of 4.7 % for the lowest density. Also interesting is to look at the shift of the lower curve with respect to the upper curve. In doing so we assume that the Hall transition occurs at a local filling factor, while the R_{xx} transition occurs at some sort of averaged filling factor over the whole Hall bar. Twice this shift should give an approximate value for the gradient. In this case using $2 \cdot \Delta\nu/\nu$ also results in a gradient of 4.7 %.

In *Table* 4.1 the same results for the other densities are shown. Notice how close the results of both methods are. From this it follows that the Hall bar is the most homogeneous at $n_e = 1.8 \times 10^{15}$ m^{-2}.

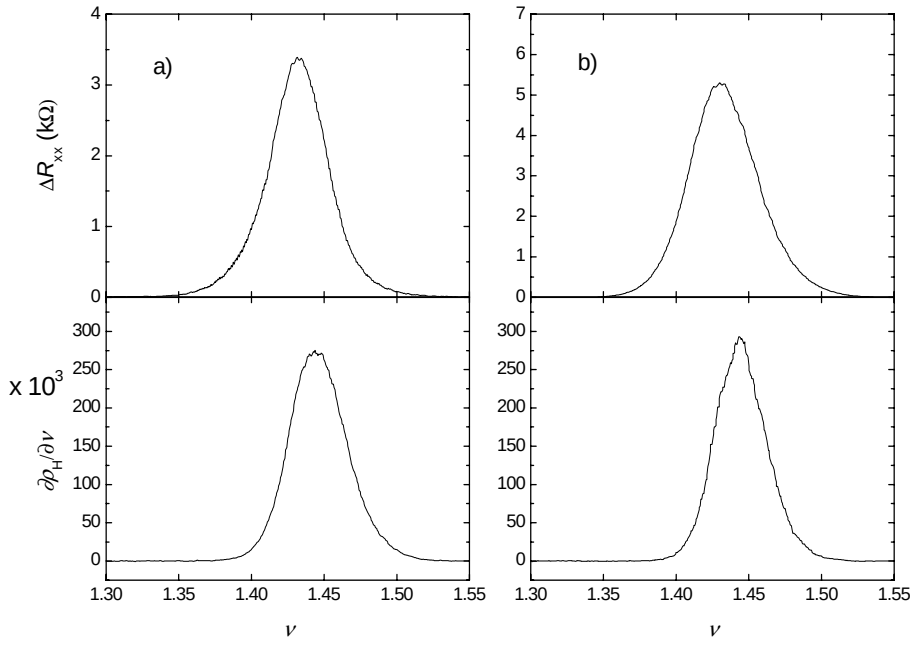

Figure 4.3 ΔR_{xx} for both field polarities (top) and slope of ρ_H (bottom) versus filling factor at $T = 100$ mK for a) $n_e = 1.8 \times 10^{15}$ m^{-2} and b) $n_e = 2.0 \times 10^{15}$ m^{-2}.

The density gradients obtained from the analysis in *Figs*. 4.2 and 4.3 for the different densities are listed in *Table* 4.1.

Table 4.1 Density gradients for the four different densities

n_e (m^{-2})	Gradient (%) reflection symmetry	Gradient (%) shift between ΔR_{xx} and $\delta\rho_H/\delta\nu$ curves
1.0×10^{15}	4.7	4.7
1.3×10^{15}	3.0	2.4
1.8×10^{15}	1.4	1.7
2.0×10^{15}	1.8	1.8

Another way of estimating the gradient is by simulating the PP-transition numerically [11]. Since a gradient causes a difference between the R_{xx}^t and R_{xx}^b curve, we can simulate a transition using the parameters obtained from the experiment (T_0, κ) and vary the gradient

until we get a result similar to the experimentally obtained curves. The measured PP transitions for the four different densities are presented in *Fig*. 4.4. Simulations using the equations shown in [21] are presented in *Fig*. 4.5. The gradients here are 2.5 % and 5 %. More about simulations will be discussed in section 4.4.

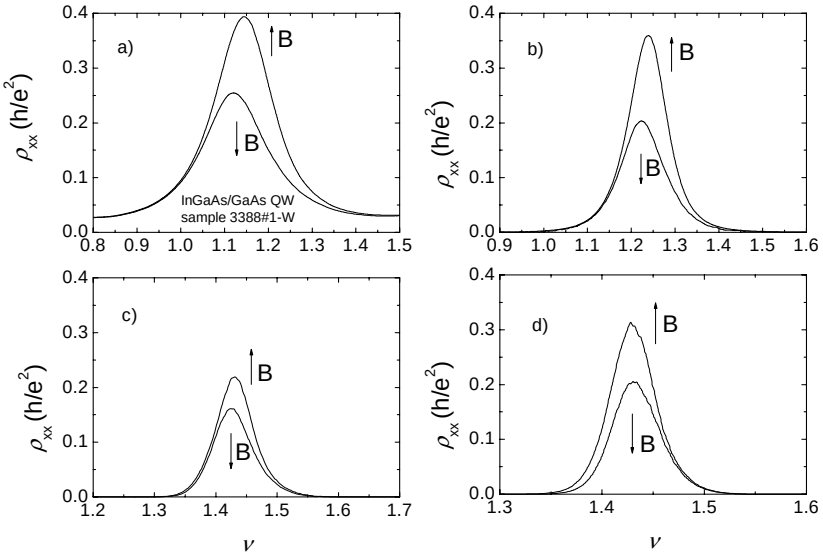

Figure 4.4 ρ_{xx} at the PP transition 2 → 1 for positive and negative field for a) n_e = 1.0 × 10^{15} m^{-2}, b) n_e = 1.3 × 10^{15} m^{-2}, c) n_e = 1.8 × 10^{15} m^{-2} and d) n_e = 2.0 × 10^{15} m^{-2}. T = 100 mK.

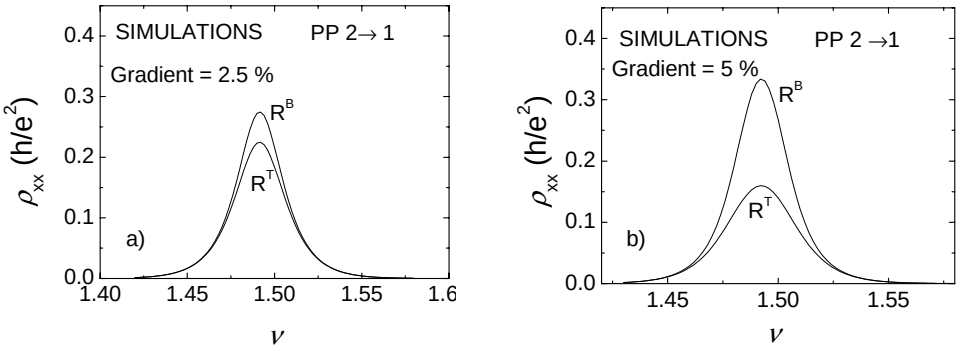

Figure 4.5 Numerical simulation of ρ_{xx} at the PP transition 2 → 1 for a) 2.5 % and b) 5 %.

First of all it should be noticed that in both the simulated curves and the measured data the transition does not occur at the theoretically expected filling factor of 1.5. The higher the gradient, the more the actual critical filling factor deviates. This deviation however, is much smaller for the simulated cases than for the measured ones, for comparable gradients. For example if we consider $n_e = 1.8 \times 10^{15}$ m^{-2}, where the density gradient according to reflection symmetry is 1.4 %, the critical filling factor is shifted to 1.43, whereas in the simulated case (2.5 %) it is only shifted to 1.49. Now consider the ratio of the maximum peak values for the different densities as shown in *Table* 4.2.

Table 4.2 Ratio of maximum peak values of $R_{xx,max}$ (B↑) /$R_{xx.max}$ (B↓) for the four measured densities and the two simulated gradients.

n_e (m^{-2})	$R_{xx,max}$ (B↑) /$R_{xx.max}$ (B↓)	Gradient (%) (simulated)	$R_{xx,max}$ (B↑) /$R_{xx.max}$ (B↓)
1.0×10^{15}	1.6	2.5	1.2
1.3×10^{15}	1.8	5	2.0
1.8×10^{15}	1.4		
2.0×10^{15}	1.6		

The ratio $R_{xx,max}$ (B↑) /$R_{xx.max}$ (B↓) follows the same trend as seen in the previously discussed methods, being the lowest for the third density and then increasing slightly for the highest density. From *Table* 4.2 we can conclude that there is a correspondence between simulations and experiment. Summarizing we can say that we have approximated the inhomogeneous nature of the 2DEG by a density gradient along the current direction of the Hall bar and that we have tried to determine this gradient in three different ways from the PP-transition: From reflection symmetry, from the shift in filling factor between the transitions of the Hall and longitudinal resistance and by making use of numerical simulations. The answers obtained from all three methods correspond with each other.

4.3 The PI-transition

In the previous paragraph we showed curves of magnetotransport data taken on the 2DEG before it reached the insulating state. This has been done only for the lowest temperature measured (100 mK). We did not consider any temperature dependence of the slope of the plateau-plateau transitions of ρ_H or the width of the peaks of the longitudinal resistance,

since in the past it turned out that these transitions are not suited for investigating critical behavior. The universal critical behavior is too much affected by sample dependent aspects like inhomogeneities in the electron density of the 2DEG. It has also been shown that for the PI-transition it is possible to disentangle the universal critical behavior from sample dependent aspects [11,12]. In this section we will examine the PI transition for all four measured densities. The resistivity near the critical filling factor ν_c follows the empirical law [11,15,20]:

$$\ln(\rho_{xx}/\rho_{xx,c}) = -\Delta\nu/\nu_0(T) \tag{4.11}$$

where:

$$\nu_0(T) = (T/T_0)^{\kappa} \tag{4.12}$$

Figs. 4.6 and 4.7 show the longitudinal resistance near the PI transition on a semi-log plot, both as a function of the filling factor and the magnetic field for $n_e = 1.8$ and 2.0×10^{15} m^{-2}. By plotting the resistivity in this way we can directly extract $\nu_0(T)$ from the slope of the curves near ν_c.

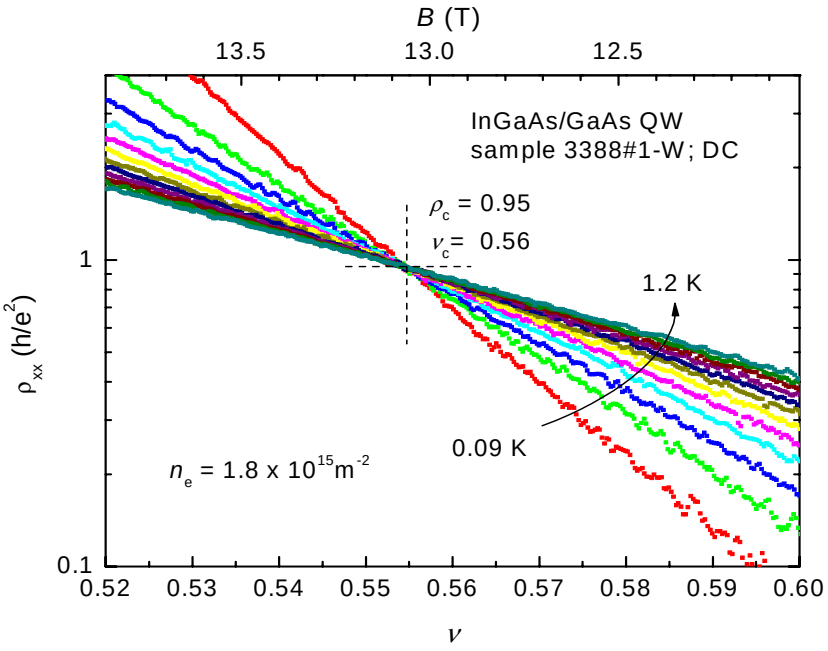

Figure 4.6 The longitudinal resistance in the regime of the PI transition for twelve different temperatures: 0.09, 0.2, 0.3, 0.4, 0.5, 0.6, 0.7, 0.8, 0.9, 1.0, 1.1 and 1.2 K as a function of filling factor (lower axis) and magnetic field (upper axis). The crossing point indicates the location of the PI-transition. The electron density is 1.8×10^{15} m^{-2}. $I = 10$ nA.

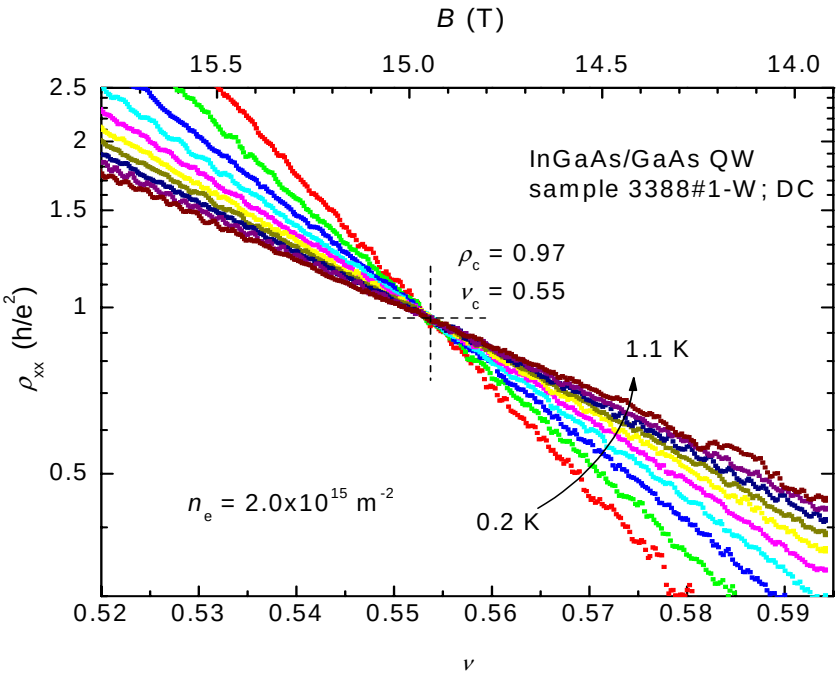

Figure 4.7 The longitudinal resistance in the regime of the PI-transition for ten different temperatures: 0.2, 0.3, 0.4, 0.5, 0.6, 0.7, 0.8, 0.9, 1.0, and 1.1 K as a function of filling factor (lower axis) and magnetic field (upper axis). The crossing point indicates the location of the PI-transition. The electron density is 2.0×10^{15} m^{-2}, $I = 10$ nA.

Data for the lowest two measured densities (1.0 and 1.3×10^{15} m^{-2}) are not shown. The value of $\rho_{xx,c}$ deviates up to 6% from the ideal value of h/e^2. This deviation is explained by sample inhomogeneities. Indeed as the density increases and the sample becomes more homogeneous, the value of $\rho_{xx,c}$ shifts towards its ideal value. Plotting the inverse of the slope of the resistivity curves (ν_0) in the vicinity of the PI-transition as function of the temperature on a log-log plot illustrates its critical behavior.

In *Fig*. 4.8 this is shown for four densities. The slopes of the curves are: 0.43 for the lowest two and 0.53 for the highest two densities.

A comparison between the curves that we obtained and the ones obtained by Ponomarenko [11] on Hall-bar 3388#1, with a geometrical factor of 5.2 is shown in *Fig*. 4.9. The values of ν_0 coincide better for the highest density.

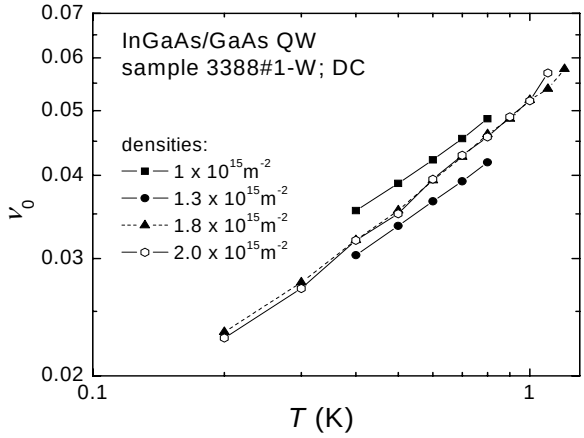

Figure 4.8 Temperature dependence of ν_0 for four different electron densities.

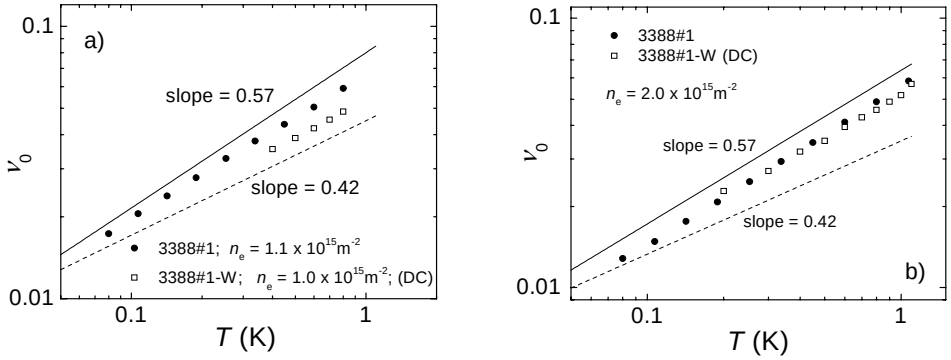

Figure 4.9 Comparison of the Temperature variation of ν_0 for sample 3388#1-W and 3388#1 [2], a) for $n_e \approx 1.0 \times 10^{15}$ m^{-2}, b) for $n_e = 2.0 \times 10^{15}$ m^{-2}. The straight lines representing slopes of 0.57 and 0.42 are given as a guide to the eye only.

4.4 Simulating the PI-transition

Hall-bars in practice turn out to be non-ideal. This means that in an attempt to measure universal properties, like critical exponents, there will always be some unwanted influences of sample-dependent (and thus non-universal) aspects. As discussed in section 4.2 one of the main disturbing factors in probing critical behavior are so called macroscopic sample inhomogeneities. In the simplest approach the inhomogeneity is a density gradient in the length direction of the Hall-bar. Making use of numerical simulations we are able to determine the influences of these inhomogeneities on the measured critical behavior. For the simulations we used software written by L.A. Ponomarenko [11], which allows

simulating a gradient in the electron density of the 2DEG. The gradient can be defined both in the direction parallel to the current flow (along the Hall bar) or perpendicular to the current flow. The Hall bar used in the simulations can be represented as follows:

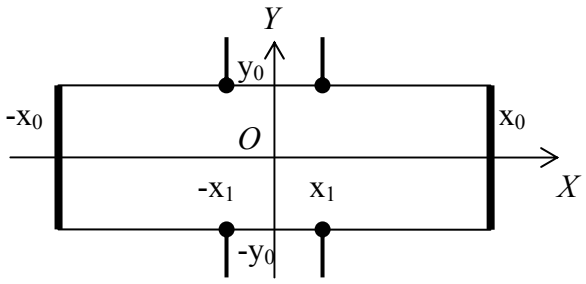

Figure 4.10 Representation of Hall bar used in numerical simulations.

The dimensions taken for the Hall bar are based on realistic ones. For the ratio between length, width and distance between the pair of Hall contacts we used 17:2:3. The simulations were done starting for zero gradient and then increasing the gradient between the Hall contact pairs in the x-direction up to 30%. The results are shown in *Figs*. 4.11a-c, where the behavior of ρ_{xx} is plotted near the PI transition for increasing gradient in the electron density. With increasing gradient the crossing point of the resistivity curves becomes less well defined. It spreads out due to shifting of the low temperature curves. The same is observed experimentally. The slope determined from the log-log plots on the right side starts to deviate from the 'zero-gradient' value of 0.58 with increasing gradient. This deviation however starts after a relatively high value of the gradient (>10%). As shown before [11], it confirms that the PI-transition is much less sensitive for density gradient than the PP-transitions. If the gradient exceeds a certain limit, also the resistivity values near the PI-transition are distorted.

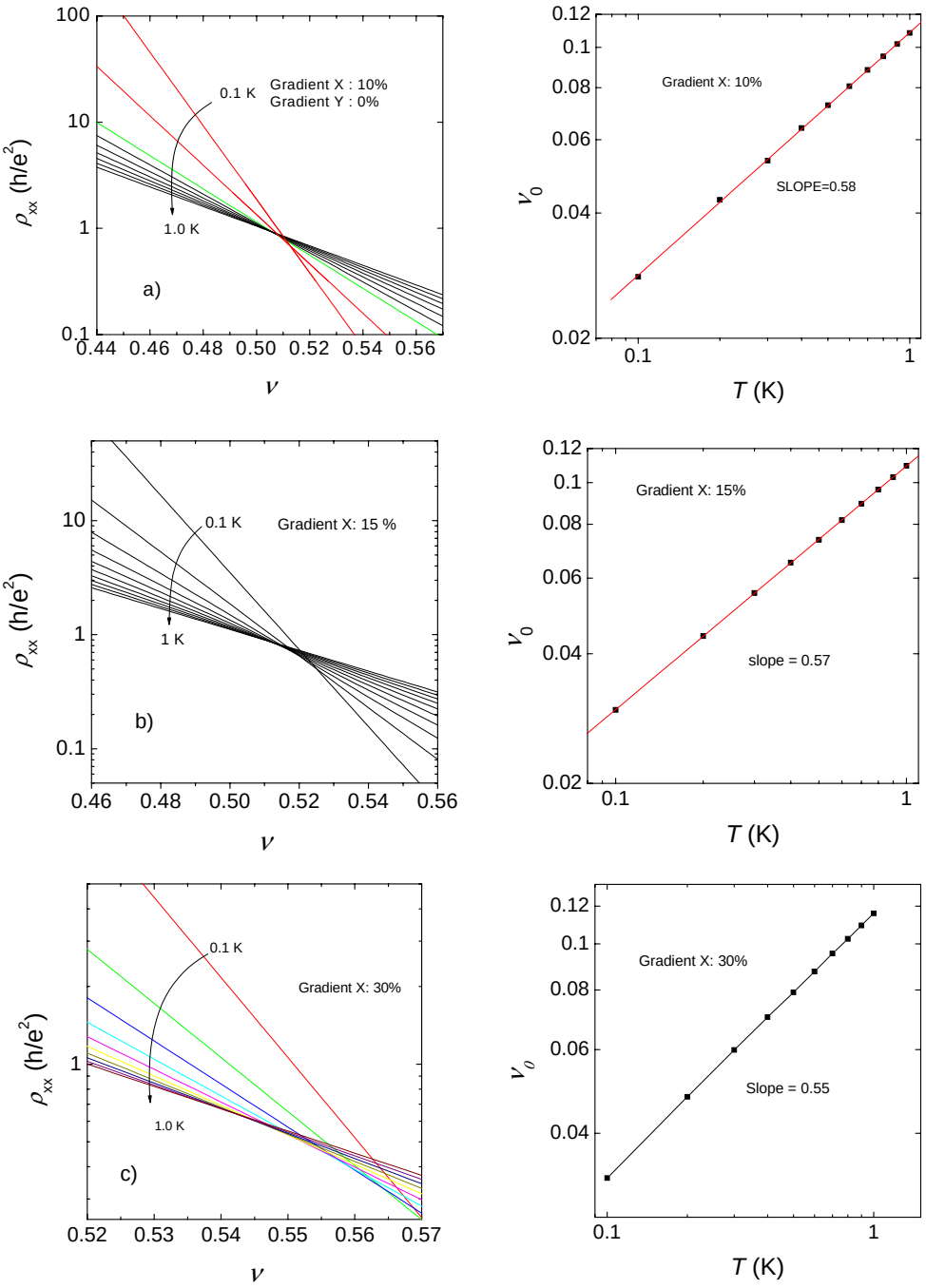

Figure 4.11 Results of numerical simulations a) 10 % gradient in x-direction b) 10 % in x-direction and c) 30 % gradient in the x-direction.

4.5 Conclusions

- Magnetotransport measurements have been carried out on an InGaAs/GaAs QW at four different electron densities tuned by illumination in the range 1.0-2.0×10^{15} m^{-2} in order to study the 2→1 PP and PI transitions.
- The density gradient in the Hall bar was determined from the 2→1 PP transition by the method of "reflection symmetry". The gradient ranges from 1.4 to 4.7 % for the investigated densities.
- The effect of the density gradient on the magnetotransport data was investigated by numerical simulations for the 2→1 PP and PI transition. The results are in good agreement with those observed in the experimental data.
- Scaling of the PI transition was investigated by extracting the temperature variation of ν_0 from the longitudinal resistance data. The critical exponent κ falls in the range 0.43-0.53. The latter value is slightly lower than the value $\kappa = 0.57$ obtain previously [11] on a narrower Hall bar prepared from the same InGaAs/GaAs wafer.

4.6 References

[1] K. von Klitzing, G. Dorda and M. Pepper, *Phys. Rev. Lett.* **45** (1980) 494.

[2a] H.P. Wei, D.C. Tsui, M.A. Paalanen and A.M.M. Pruisken, *Phys. Rev. Lett.* **61** (1988) 1294.

[2b] A.M.M. Pruisken, *Phys. Rev. Lett*. **61** (1988) 1297.

[3] H.P. Wei, D.C. Tsui and A.M.M. Pruisken, *Phys. Rev. B* **33** (1985) 1488.

[4] S. Koch, R.J. Haug, K. von Klitzing and K. Ploog, *Phys. Rev. Lett.* **43** (1991) 6828.

[5] R.B. Dunford, N. Griffin, M. Pepper, P.J. Phillips and T.E. Whall, *Physica E* **6** (2000) 297.

[6] J. Wakabayashi, A. Fukano, S. Kawaji, Y. Koike and T. Fukase, *Surf. Science* **229** (1990) 60.

[7] K.H. Yoo, H.C. Kwon and J.C. Park, *Solid State Commun.* **92** (1994) 821.

[8] D. Shahar, D.C. Tsui, M. Shayegan, J.E. Cunningham, E. Shimshoni and S.L. Sondhi, *Solid State Commun.* **102** (1997) 817.

[9] A.M.M. Pruisken, B. Skoric and M. Baranov, *Phys. Rev. B* **60** (1999) 16838.

[10] H.P. Wei, S.Y. Lin and D.C. Tsui, *Phys. Rev. B* **45** (1992) 3926.

[11] L.A. Ponomarenko, *Ph.D Thesis* (University of Amsterdam, 2005), unpublished.

[12] B. Karmakar, M.R. Gokhale, A.P. Shah, B.M. Arora, D.T.N. de Lang, A. de Visser, L.A. Ponomarenko and A.M.M. Pruisken, *Physica E* **24** (2004) 187.

[13] L. A. Ponomarenko, D.T.N. de Lang, A. de Visser, V.A. Kulbachinskii, G.B. Galiev, H. Künzel and A.M.M. Pruisken, *Solid State Commun.* **130** (2004) 705.

[14] D.T.N. de Lang, *Ph.D Thesis* (University of Amsterdam, 2005), unpublished.

[15] A.M.M. Pruisken, D.T.N. de Lang, L.A. Ponomarenko and A. de Visser, *Solid State Commun.* **137** (2006) 540.

[16] A. de Visser, L.A. Ponomarenko, G. Galistu, D.T.N. de Lang, A.M.M. Pruisken, U. Zeitler and D. Maude, *J.Phys. Conf. Series* (2006) Sendai.

[17] Wanli Li, G.A. Csathy, D.C. Tsui, L.N. Pfeiffer and K.W. West, *Phys. Rev. Lett*. **94** (2005) 206807.

[18] Wanli Li, G.A. Csathy, D.C. Tsui, L.N. Pfeiffer and K.W. West, *Int. Journal of Modern Physics B* **18** (2004) 3569.

[19] Wanli Li, C.L. Vicente, J.S. Xia, W. Pan, D.C. Tsui, L.N. Pfeiffer and K.W. West, *Phys. Rev. Lett*. **102** (2009) 216801.

[20] D.T.N. de Lang, L.A. Ponomarenko, A. de Visser and A.M.M. Pruisken, *Phys. Rev. B* **75** (2007) 1.

[21] J. Oswald, G. Span and F. Kuchar, *Phys. Rev. B* 58 (1998) 15401.